Electronic Supplementary Material (ESI) for RSC Advances.
This journal is © The Royal Society of Chemistry 2016

Supporting Information

For the manuscript titled

Qualitative Analysis of Some Alkanethiols on Au Nanoparticles during SERS

R. A. Harris*[1], M. Mlambo[2], P. S. Mdluli[3]

[1] University of the Free State, Physics Department, Nelson Mandela Drive, Bloemfontein, South Africa, 9301

[2] University of Pretoria, Physics Department, Pretoria, 0002, South Africa

[3] Durban University of Technology, Department of Chemistry, P O Box 1334, Durban, 4000, South Africa

*Corresponding author email: harrisra@ufs.ac.za; raharrisphd@gmail.com

Table of Contents

Experimental S4

Materials S4

Instrumentation S4

Synthesis, functionalization and conjugation of Au nanoparticles S5

Synthesis of citrate gold nanoparticles S5

Functionalization of gold nanoparticles S5

Calculation of Enhancement Factor S5

Computational Details S6

Figure S1: Molecular structure of the different surfactants used in this study S7

Results and Characterization S9

Table S1: Summary of SPR bands S9

Figure S2: DFT calculated Raman spectra S10

Figure S3: TEM images of AuNPs with 1% and 50% HS-$(CH_2)_{11}$- NHCO-coumarin S11

Figure S4: Raman spectra of AuNPs with HS-$(CH_2)_{11}$- NHCO-coumarin S11

Figure S5: TEM images of AuNPs with 1% and 50% HS-$(CH_2)_{11}$-triphenylimidazole. S12

Figure S6: Raman spectra of AuNPs with HS-$(CH_2)_{11}$-triphenylimidazole. S12

Figure S7: TEM images of AuNPs with 1% and 50% HS-$(CH_2)_{11}$-indole. S13

Figure S8: Raman spectra of AuNPs with HS-$(CH_2)_{11}$-indole. S13

Figure S9: TEM images of AuNPs with 1% and 50% HS-$(CH_2)_{11}$- hydroquinone S14

Figure S10: Raman spectra of AuNPs with HS-$(CH_2)_{11}$- hydroquinone. S14

Figure S11: Absorption spectra of different AuNPs with HS-$(CH_2)_{11}$-NHCO-Coumarin. S15

Figure S12: Absorption spectra of different AuNPs with HS-$(CH_2)_{11}$-triphenylimidazole. S15

Figure S13: Absorption spectra of different AuNPs with HS-$(CH_2)_{11}$-indole. S15

Figure S14: Absorption spectra of different AuNPs with HS-$(CH_2)_{11}$-hydroquinone. S16

Figure S15: Molecule-to-surface orientation for AuNPs with PEG/Coumarin. S16

Figure S16: Molecule-to-surface orientation for AuNPs with PEG/Coumarin. S17

Figure S17: Molecule-to-surface orientation for AuNPs with PEG/Coumarin. S17

Figure S18: Molecule-to-surface orientation for AuNPs with PEG/Coumarin. S18

References S18

1. Experimental

1.1 Materials

Hydrogen tetrachloroaurate trihydrate (Sigma- Aldrich 99.9%), tri-sodium citrate (ACE AR, 99%), HS-PEG-$(CH_2)_{11}$COOH, HS-PEG-$(CH_2)_{11}$-OH, HS-$(CH_2)_{11}$-NHCO-coumarin, HS-$(CH_2)_{11}$-Triphenylimidazole, HS-$(CH_2)_{11}$-indole, HS-$(CH_2)_{11}$-hydroquinone were obtained from ProChimia Surfaces (Poland).

1.2 Instrumentation

High purity water with resistivity of 18.1 ΩM was obtained from a Milli-Q Advantage water system purchased from Millipore (USA) and was used in all the experiments. Samples were purified using Hettich MIKRO 22R centrifuge.

Absorption spectra of AuNPs were recorded on a Lambda 35 UV-Vis spectrometer. Maximum absorption wavelength was determined by calculating the wavelength at which

$$\frac{dA}{d\lambda} = 0 \tag{1}$$

where A = absorbance and λ = absorption wavelength.

Transmission electron microscope (TEM) images were obtained using a JEM-2100F at 200 kV. The TEM grids were prepared by depositing approximately 10 µl of the solution obtained after centrifugation and allowed to dry in air.

Raman spectra were acquired using a PerkinElmer Raman Station 400 benchtop Raman spectrometer. The excitation source was a near-infrared 785 nm laser (100mW at the sample), with a spot size of 100 µm. A spectral range of 100-3200 cm^{-1} was employed. The detector was a temperature controlled Charged Coupled Device (CCD) detector (-50 °C) incorporating a 1024 x 256 pixel sensor. Spectra were acquired using Spectrum software and images were acquired using Spectrum IMAGE software, both supplied by PerkinElmer (Bucks, UK).

1.3 Synthesis, functionalization and conjugation of Au nanoparticles

1.3.1 Synthesis of citrate gold nanoparticles

In a typical experimental procedure, an aqueous solution of tri-sodium citrate (0.04 M) was added to a boiling aqueous solution of tetrachloroaurate (250 mL, 1 mM). The mixture was allowed to boil for five minutes while vigorous stirring, then the mixture was removed from heat and continued stirring for a further three hours. To obtain different sizes of AuNPs, the volume of tri-sodium citrate aqueous solution was varied.

1.3.2 Functionalization of gold nanoparticles [1, 2]

The resulting different sizes of AuNPs were filtered, and then 40 mL [Optical Density (OD) = 1, 0.73 nM] aliquots of each size (AuNPs) were treated with 200 µl of HS-$(CH_2)_{11}$-PEG-COOH (8 mg/mL). Each 40 mL aliquot of the AuNPs coated with HS-$(CH_2)_{11}$-PEG-COOH, were further divided into two aliquots of 20 mL each, to be co-stabilized with different percentages of HS-$(CH_2)_{11}$-NHCO-coumarin (1% or 50%, respectively). For AuNPs stabilized with 1% HS-$(CH_2)_{11}$-NHCO-coumarin, 0.02 mg of HS-$(CH_2)_{11}$-NHCO-coumarin was dissolved in 1 mL of methanol and then thoroughly mixed with HS-$(CH_2)_{11}$-PEG-COOH (1.98 mg) in 1 mL of methanol. For stabilization with 50 % HS-$(CH_2)_{11}$-NHCO-coumarin, 1 mg of each alkanethiols was dissolved in methanol and swirled for few minutes. The mixtures of different percentages (1% and 50% HS-$(CH_2)_{11}$-NHCO-coumarin) were each added to 20 mL of AuNPs, and stirred at 800 rpm for three hours, at room temperature. Similar procedure was followed for the preparation of AuMMPCs using other Raman active alkanethiols i.e.; HS-$(CH_2)_{11}$-Triphenylimidazole, HS-$(CH_2)_{11}$-indole and HS-$(CH_2)_{11}$-hydroquinone.

1.3.3 Calculation of Enhancement Factor

The enhancement factor (EF) was calculated as follows. Firstly, all sample collection and handling conditions were kept invariant throughout all the measurements, i.e. the laser power, accumulation time, and exposure time. Under these conditions, the EF can be calculated with:

$$EF = \left(\frac{I_{surf}}{I_{bulk}}\right) \times \left(\frac{N_{bulk}}{N_{surf}}\right) \quad (1)$$

where I_{surf} and I_{bulk} are intensities of the vibrational mode in the SERS and the vibrational mode in the Raman spectrum, respectively[3]. N_{bulk} is the number of molecules that are probed on the

Raman spectrum (free HS-$(CH_2)_{11}$-NHCO-coumarin for example), while N_{surf} is the number of molecules probed using SERS (HS-$(CH_2)_{11}$-NHCO-coumarin with Au substrate for example). N_{bulk} can be further expanded into:

$$N_{bulk} = \frac{A \times h \times \rho}{m} \tag{2}$$

where A, h, ρ, and m are the laser spot area, the focal length, the density of solid surfactant (like HS-$(CH_2)_{11}$-NHCO-coumarin for example), and its molecular weight (405,55 g/mol in the case of coumarin), respectively. N_{surf} can be expressed as:

$$N_{surf} = 4\pi r^2 CAN \tag{3}$$

where r, C, A and N are the average radius of the Au nanoparticles, the surface density of the surfactant, the area of the laser spot, and the surface coverage of the Au nanoparticles (particles μm^{-2}), respectively. Thus, by using equations (2) and (3), the enhancement factor (EF) can be expressed as:

$$EF = \left(\frac{I_{surf}}{I_{bulk}}\right) \times \left(\frac{Ah\rho}{4\pi m r^2 CAN}\right) \tag{4}$$

This equation (4) was used to calculate the enhancement factor from the measured intensities of υ(C-H).

(The focal length was used to calculate the area of a laser spot which was assumed to be cylindrical, using the cylinder area formula:

$$A = 2\pi r^2 + 2\pi r h \tag{5}$$

Where r is the radius of the laser spot and h is the focal length.)

Computational Details

By using the '*adsorption locator'* module of the *BioVia Materials Studio 7.0* (*MS 7.0*) software package, different ratios of the number of HS-$(CH_2)_{11}$-PEG-COOH (Figure 2 (a)) to the four thiolated coumarin molecules under investigation were adsorbed onto the nanoparticle surface. These molecules were HS-$(CH_2)_{11}$-NHCO-coumarin (Figure 2 (b)), HS-$(CH_2)_{11}$-NHCO-indole (Figure 2 (c)), HS-$(CH_2)_{11}$-triphenylimidizole (Figure 2 (d)) and HS-$(CH_2)_{11}$-hydroquinone (Figure 2 (e)). For the initial adsorption a *universal forcefield* was used and the charges were assigned using the *QEq* charge equilibration method. As a check, the same

experiment was repeated using the charge consistent valence forcefield (*cvff*) with charges assigned by the forcefield. The same results were generated, however, it was found that it was easier to visually inspect and find sulphur-gold bonds by using the *universal* forcefield at this stage of the simulations. The summation method for the electrostatics and the Van der Waals interactions were both atom based and the quality of the calculation was set to '*ultra-fine'*. This experiment was repeated several times for the following PEG to surfactant molecule ratios: 100%, 90%, 74%, 50%, 24%, 2% and 0%.

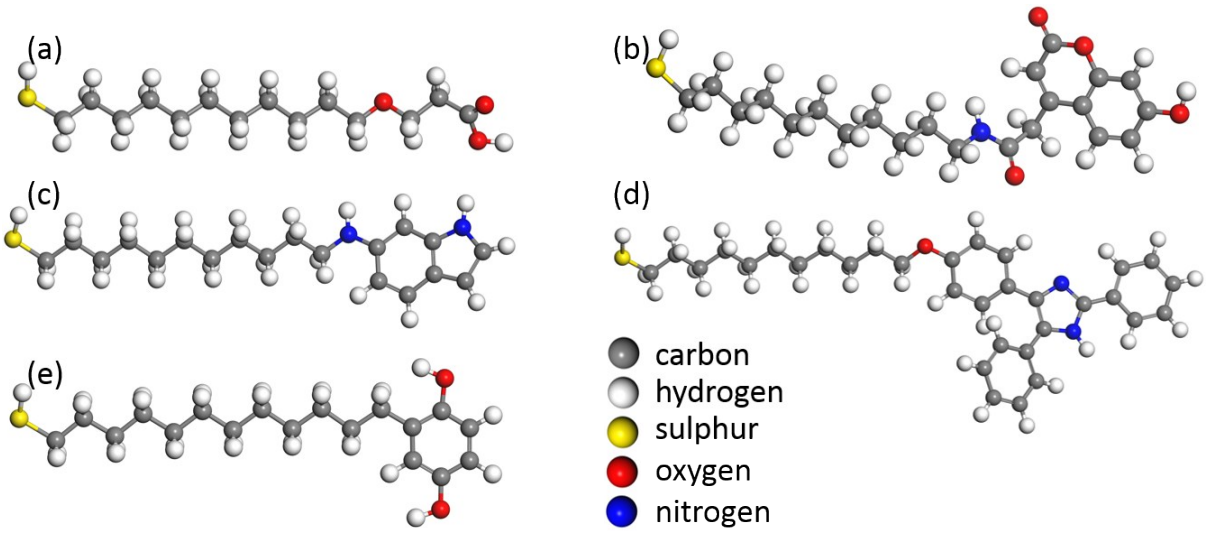

Figure S1: (*a*) HS-$(CH_2)_{11}$-PEG-COOH, (*b*) HS-$(CH_2)_{11}$-NHCO-coumarin, (*c*) HS-$(CH_2)_{11}$-NHCO-indole, (*d*) HS-$(CH_2)_{11}$-triphenylimidazole and (*e*) HS-$(CH_2)_{11}$-hydroquinone. Yellow atoms are sulphur, red = oxygen, blue = nitrogen, grey = carbon and white = hydrogen.

Molecular Mechanics (MM): Geometry optimization

Molecular mechanics were used to determine the optimum geometries for each of the resulting PEG, surfactant-nanoparticle systems. This was done by using the *Discover* – module of *MS 7.0*. The charge consistent valence forcefield (*cvff*) was used with charges assigned by the forcefield. These settings were applied to both Van der Waals and Coulomb forces and the summation method was atom based. The minimization method was selected as '*smart'*, which uses combinations of the *steepest descent, conjugate gradient* and *newton methods*. For the *conjugate gradient* method, the *Fletcher-Reeves* algorithm was used and for the *newton method* the *Broyden–Fletcher–Goldfarb–Shanno (BFGS)* algorithm was used.

Molecular Dynamics

After geometry optimization by MM, molecular dynamics simulations were performed on each of the aforementioned systems to arrive at the final, energy-optimized systems. A *NVT* ensemble at room temperature was used with a time step of 1.0 femtoseconds and a dynamic time of 20.0 picoseconds. An *Anderson*-thermostat was used with a collision ratio of 1.0 and the number of simulation steps were 20 000.

Binding Energy

In order to calculate the binding energies between the surfactants (E_s) (PEG and all four alkanethiols) and the nanoparticle (E_{np}) surface, it is well known that the total energy ($E_{totalsystem}$) is the sum of the total energy of each separate system plus the interaction energy between the nanoparticle and the surfactants. Thus the binding energy (E_b) is calculated according to the following equation[4]:

$$E_b = (E_{totalsystem}) - E_{np} - E_s \quad (1)$$

The total energy of the surfactants is calculated according to the following procedure: after the optimum configuration of the nanoparticle-surfactants system was determined, the nanoparticle was removed from the system. Then a single point energy calculation as carried out, from which the total energy of the surfactant was determined. In order to calculate the total energy of the nanoparticle, the surfactants were removed and a single point energy calculation was carried out to get the total energy of the nanoparticle.

Density Functional Theory (DFT)

To investigate the molecular structure, orbitals, electron density, electrostatic potential as well as the electro- and nucleophilic centres of each molecule, calculations were done within the framework of the *density functional theory* as implemented in the *DMOL3* code of *BioVia Materials Studio* 8.0 using the exchange-correlation function proposed by Perdew−Wang (*PW91*) within the Generalized Gradient Approximation (*GGA*). An all-electron core treatment was implemented with d-orbital and p-orbital polarization (*DNP* basis set). This basis set uses double-numerical basis functions together with polarization functions. The numerical integration were performed on a real space grid with an equivalent energy cut-off set to 3400 eV. The calculations were considered to be converged when the force on each ion was less than 0.001eV/Å, and a total energy convergence criterion of 10^{-5} eV was set.

2. Results and characterization

Sample		SPR (nm)	O.D.
	Au14nm	519	1.14
	Au30nm	528	1.21
	Au40nm	529	1.04
Coumarin	Au14 1%	523	1.25
	Au14 50%	525	1.33
	Au30 1%	533	1.29
	Au30 50%	533	1.26
	Au40 1%	534	1.02
	Au40 50%	534	1.1
TPI	Au14 1%	525	1.31
	Au14 50%	527	1.4
	Au30 1%	533	1.33
	Au30 50%	533	1.34
	Au40 1%	533	1.11
	Au40 50%	536	0.89
HSI	Au14 1%	524	1.29
	Au14 50%	526	1.34
	Au30 1%	532	1.75
	Au30 50%	533	1.41
	Au40 1%	532	1.11
	Au40 50%	537	0.88
HQ	Au14 1%	524	0.9
	Au14 50%	524	0.9
	Au30 1%	532	1.73
	Au30 50%	532	1.71
	Au40 1%	532	1.09
	Au40 50%	532	1.09

Table S1: Summary of SPR bands of AuNPs and AuMMPCs (mixed monolayer protected clusters). (Coumarin: HS-$(CH_2)_{11}$-NHCO-coumarin, TPI: HS-$(CH_2)_{11}$- triphenylimidazole, HIS: HS-$(CH_2)_{11}$- NHCO-indole, and HQ: HS-$(CH_2)_{11}$-hydroquinone).

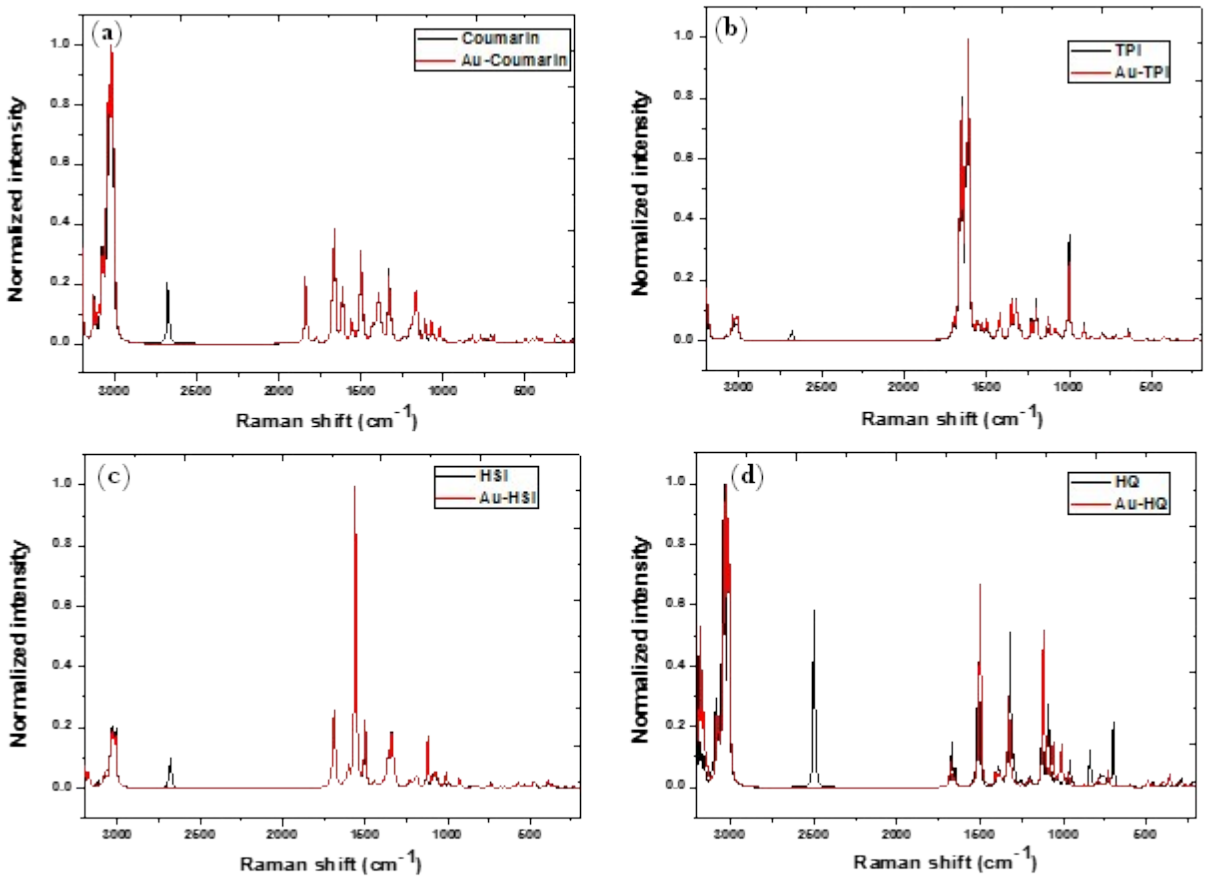

Figure S2: DFT calculated Raman spectra of AuMMPCs of (a) HS-$(CH_2)_{11}$-NHCO-coumarin, (b) HS-$(CH_2)_{11}$-triphenylimidazole, (c) HS-$(CH_2)_{11}$-indole and (d) HS-$(CH_2)_{11}$-hydroquinone

Ligands	Citrate	1% Raman reporter	50% Raman reporter
Sizes 14 nm	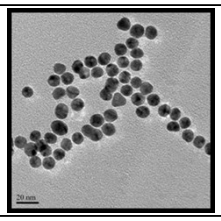	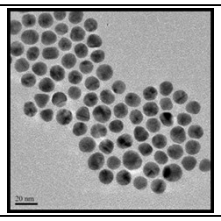	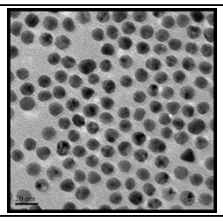
30 nm	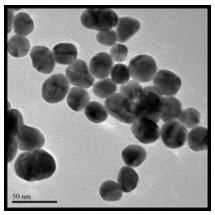	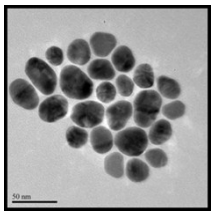	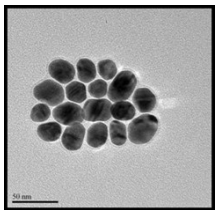
40 nm	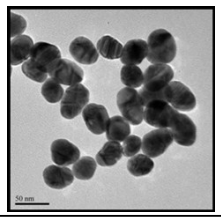	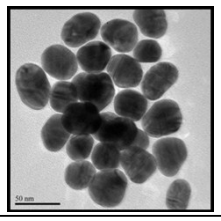	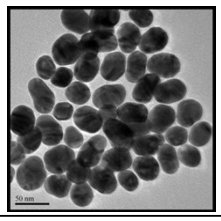

Figure S3: TEM images of AuNPs and their corresponding AuMMPCs of 1% and 50% of HS-$(CH_2)_{11}$- NHCO-coumarin.

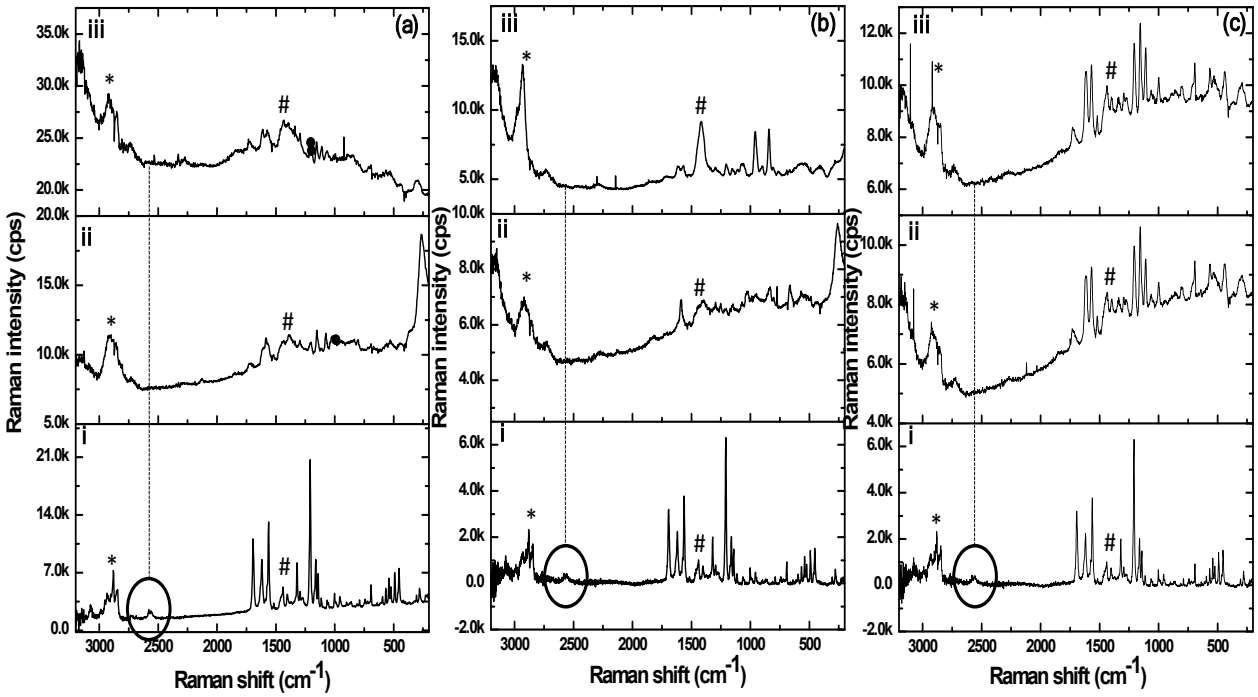

Figure S4: Raman spectra of AuMMPCs of different stoichiometric ratios of HS-$(CH_2)_{11}$-NHCO-coumarin prepared with different AuNPs sizes (a) 14 nm, (b) 30 nm, and (c) 40 nm. The circled peak is the vibrational band of S-H, (* and #) denotes the symmetric and asymmetric bands of C-H bonds. (i) HS-$(CH_2)_{11}$-NHCO-coumarin, (ii) 1% HS-$(CH_2)_{11}$-NHCO-coumarin and (ii) 50% HS-$(CH_2)_{11}$-NHCO-coumarin.

Ligands	Citrate	1% Raman reporter	50% Raman reporter
Sizes 14 nm	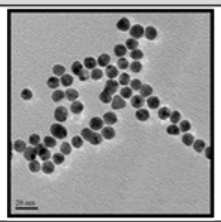	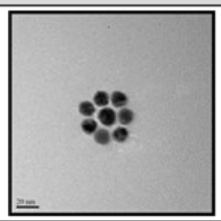	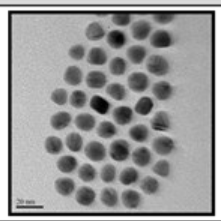
30 nm	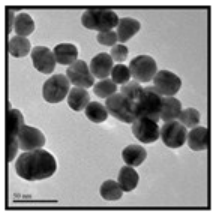	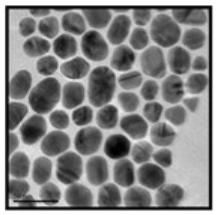	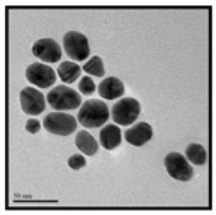
40 nm	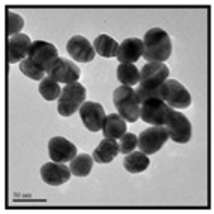	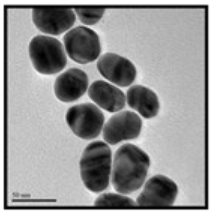	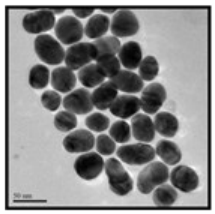

Figure S5: TEM images of AuNPs and their corresponding AuMMPCs of 1% and 50% of HS-$(CH_2)_{11}$-triphenylimidazole.

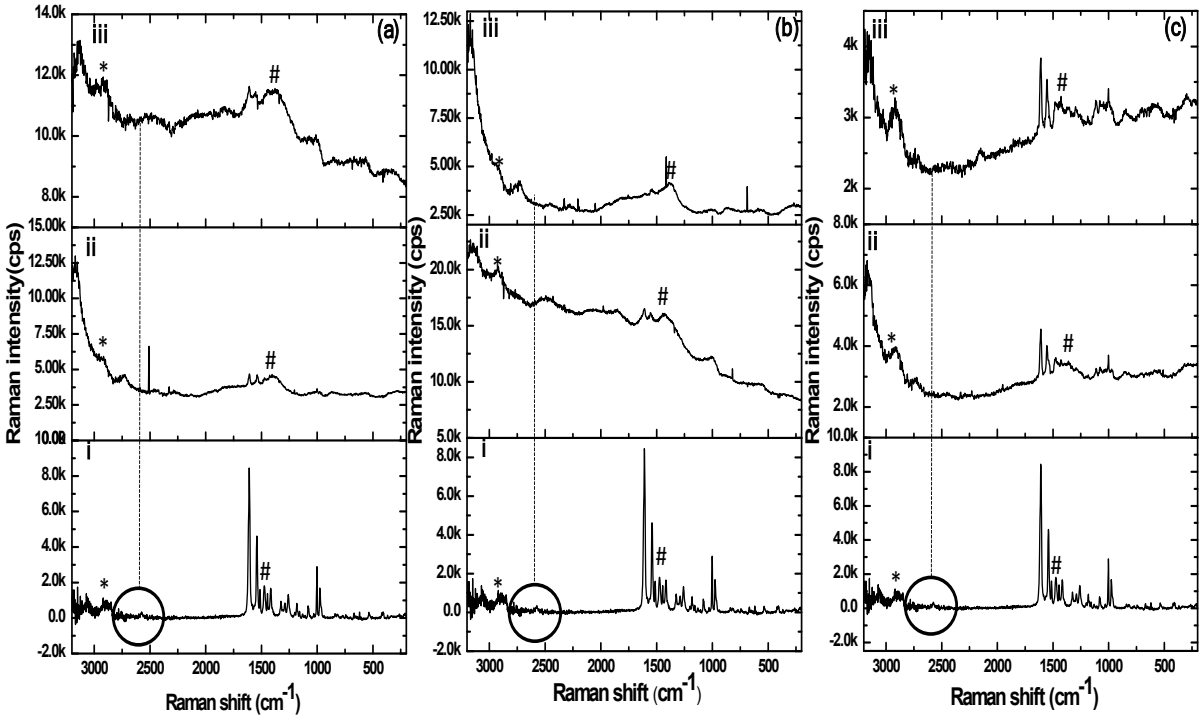

Figure S6: Raman spectra of AuMMPCs of different stoichiometric ratios of HS-$(CH_2)_{11}$-triphenylimidazole prepared with different AuNPs sizes (a) 14 nm, (b) 30 nm, and (c) 40 nm. The circled peak is the vibrational band of S-H, (* and #) denotes the symmetric and asymmetric bands of C-H bonds. (i) HS-$(CH_2)_{11}$-triphenylimidazole, (ii) 1% HS-$(CH_2)_{11}$-triphenylimidazole and (ii) 50% HS-$(CH_2)_{11}$-triphenylimidazole.

Ligands	Citrate	1% Raman reporter	50% Raman reporter
Sizes 14 nm	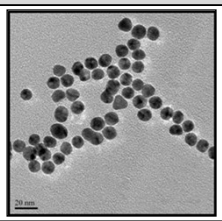	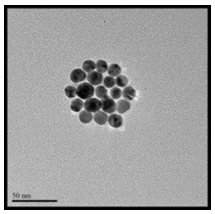	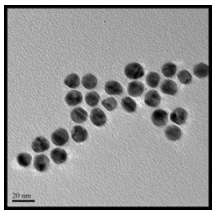
30 nm	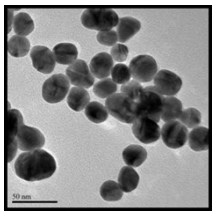	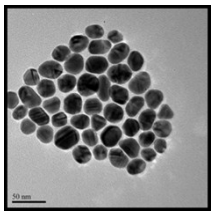	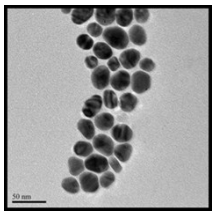
40 nm	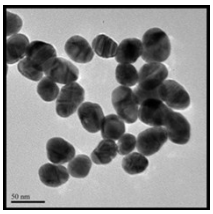	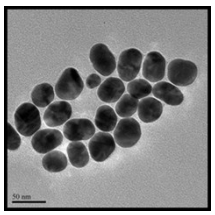	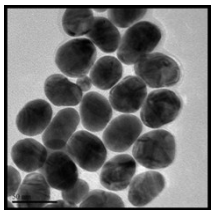

Figure S7: TEM images of AuNPs and their corresponding AuMMPCs of 1% and 50% of HS-$(CH_2)_{11}$-indole.

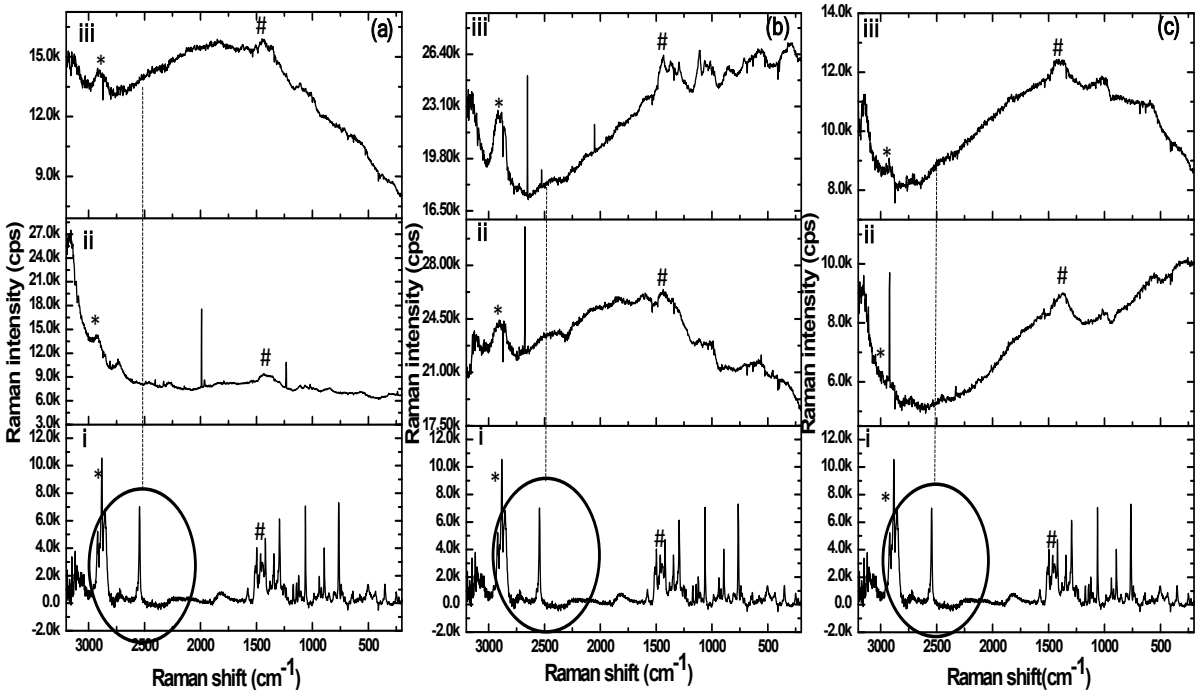

Figure S8: Raman spectra of AuMMPCs of different stoichiometric ratios of HS-$(CH_2)_{11}$-indole prepared with different AuNPs sizes (a) 14 nm, (b) 30 nm, and (c) 40 nm. The circled peak is the vibrational band of S-H, (* and #) denotes the symmetric and asymmetric bands of C-H bonds. (i) HS-$(CH_2)_{11}$- indole, (ii) 1% HS-$(CH_2)_{11}$- indole and (ii) 50% HS-$(CH_2)_{11}$-indole.

Ligands	Citrate	1% Raman reporter	50% Raman reporter
Sizes 14 nm	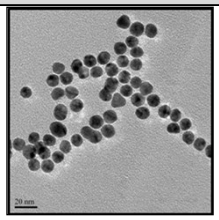	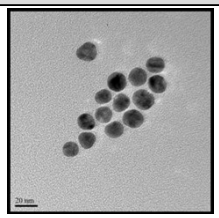	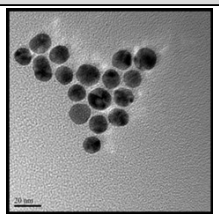
30 nm	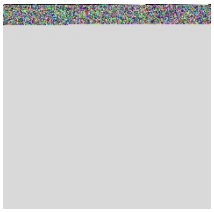	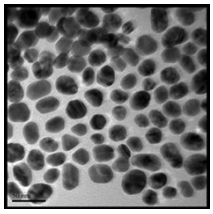	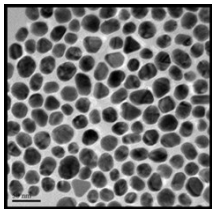
40 nm	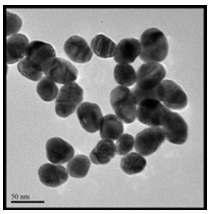	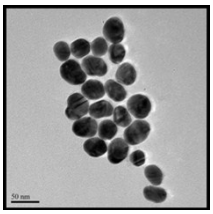	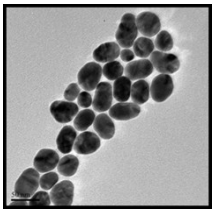

Figure S9: TEM images of AuNPs and their corresponding AuMMPCs of 1% and 50% of HS-$(CH_2)_{11}$- hydroquinone.

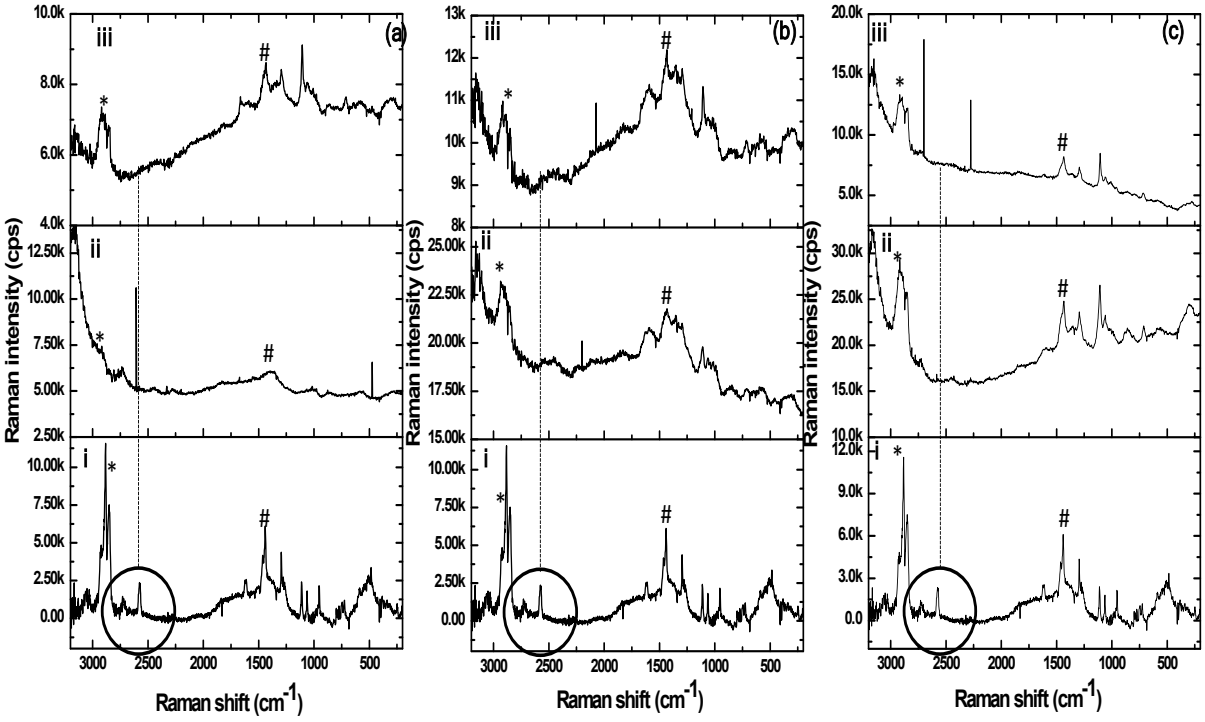

Figure S10: Raman spectra of AuMMPCs of different stoichiometric ratios of HS-$(CH_2)_{11}$-hydroquinone prepared with different AuNPs sizes (a) 14 nm, (b) 30 nm, and (c) 40 nm. The circled peak is the vibrational band of S-H, (* and #) denotes the symmetric and asymmetric bands of C-H bonds. (i) HS-$(CH_2)_{11}$- hydroquinone, (ii) 1% HS-$(CH_2)_{11}$- hydroquinone and (ii) 50% HS-$(CH_2)_{11}$- hydroquinone.

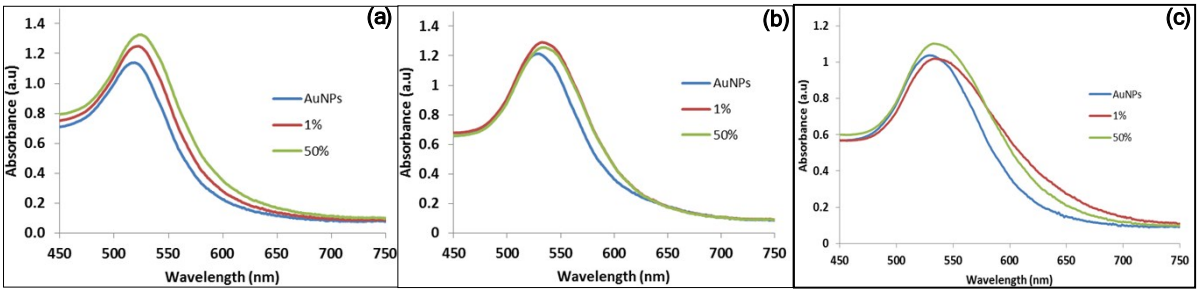

Figure S11: Absorption spectra of different AuNPs sizes with their corresponding AuMMPCs in different stoichiometric ratios of HS-$(CH_2)_{11}$-NHCO-Coumarin (a) 14 nm, (b) 30 nm and (c) 40 nm.

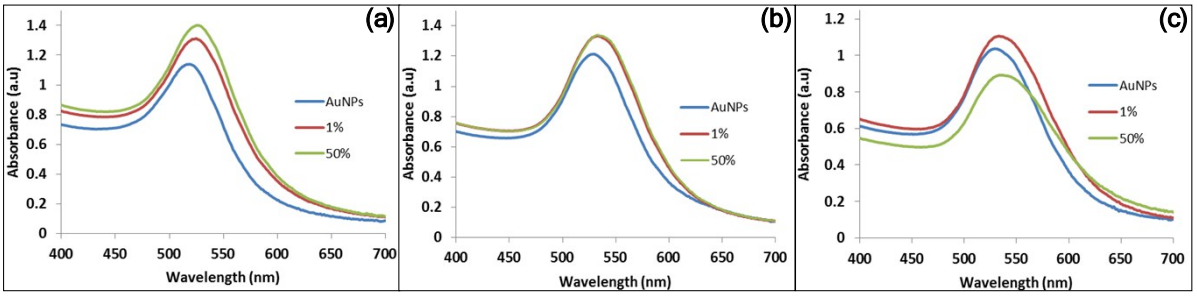

Figure S12: Absorption spectra of different AuNPs sizes with their corresponding AuMMPCs in different stoichiometric ratios of HS-$(CH_2)_{11}$-triphenylimidazole (a) 14 nm, (b) 30 nm and (c) 40 nm.

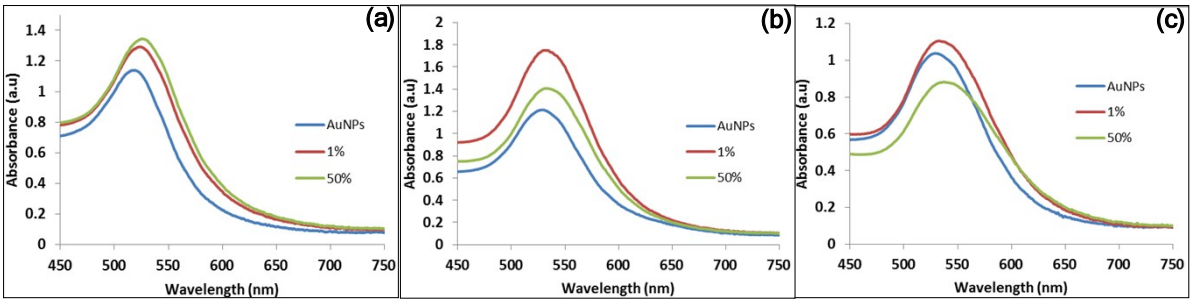

Figure S13: Absorption spectra of different AuNPs sizes with their corresponding AuMMPCs in different stoichiometric ratios of HS-$(CH_2)_{11}$-indole (a) 14 nm, (b) 30 nm and (c) 40 nm.

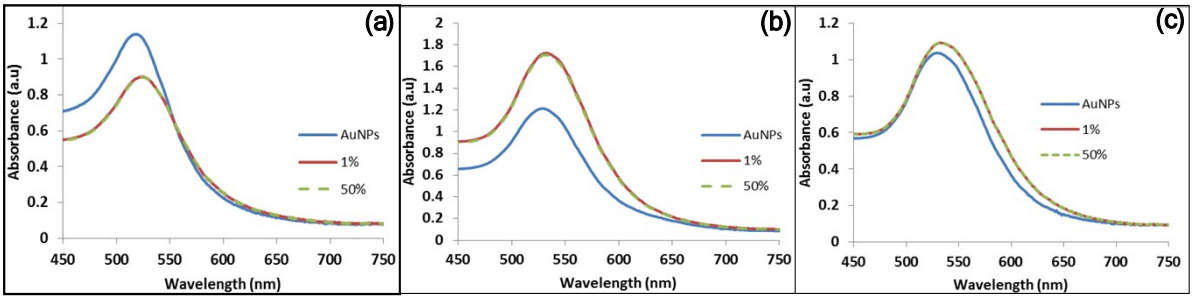

Figure S14: Absorption spectra of different AuNPs sizes with their corresponding AuMMPCs in different stoichiometric ratios of HS-$(CH_2)_{11}$-hydroquinone (a) 14 nm, (b) 30 nm and (c) 40 nm.

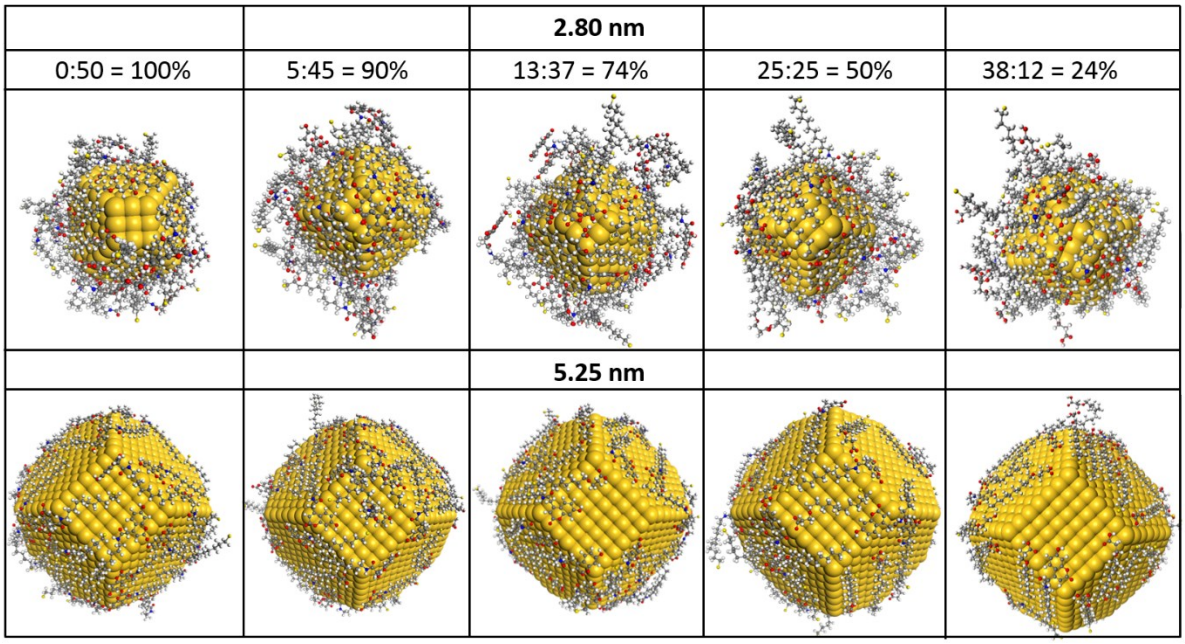

Figure S15: Relative molecule-to-surface orientation for different sized AuNPs with different ratios of PEG/Coumarin.

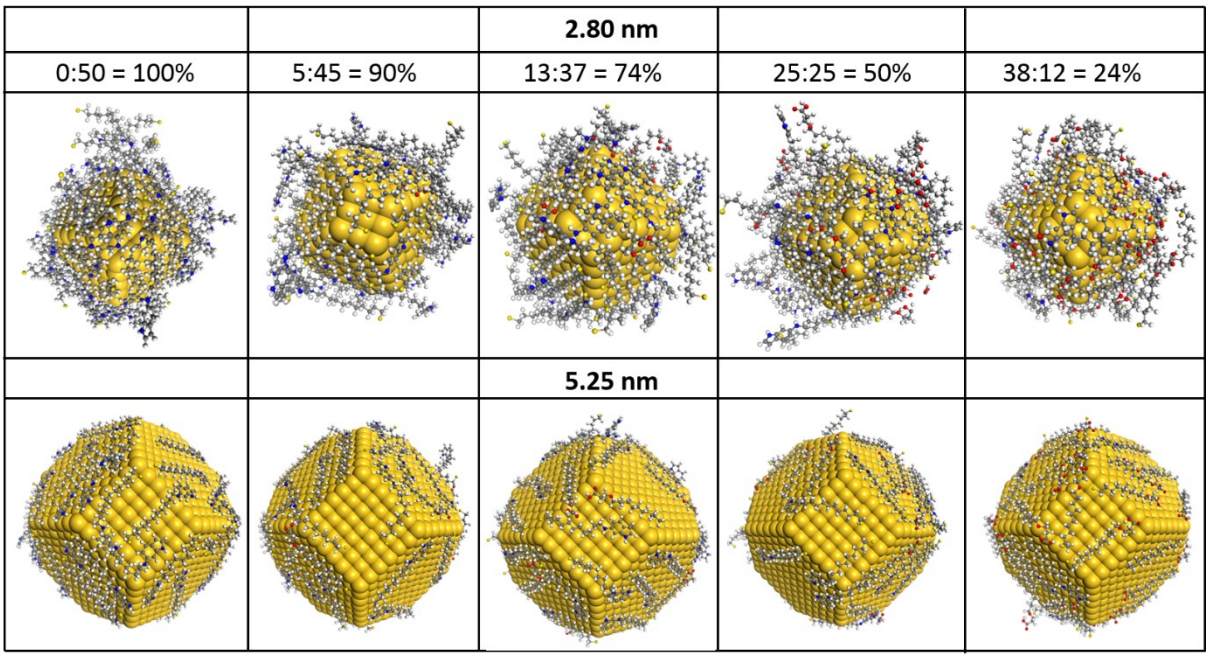

Figure S16: Relative molecule-to-surface orientation for different sized AuNPs with different ratios of PEG/Indole.

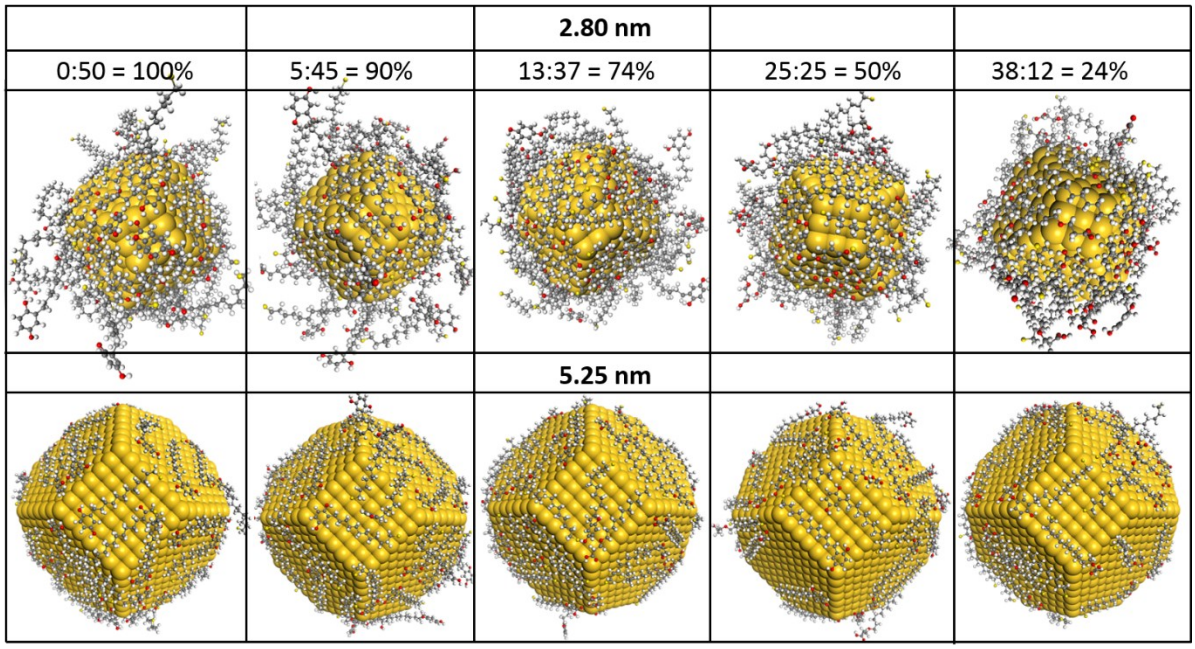

Figure S17: Relative molecule-to-surface orientation for different sized AuNPs with different ratios of PEG/Hydroquinone.

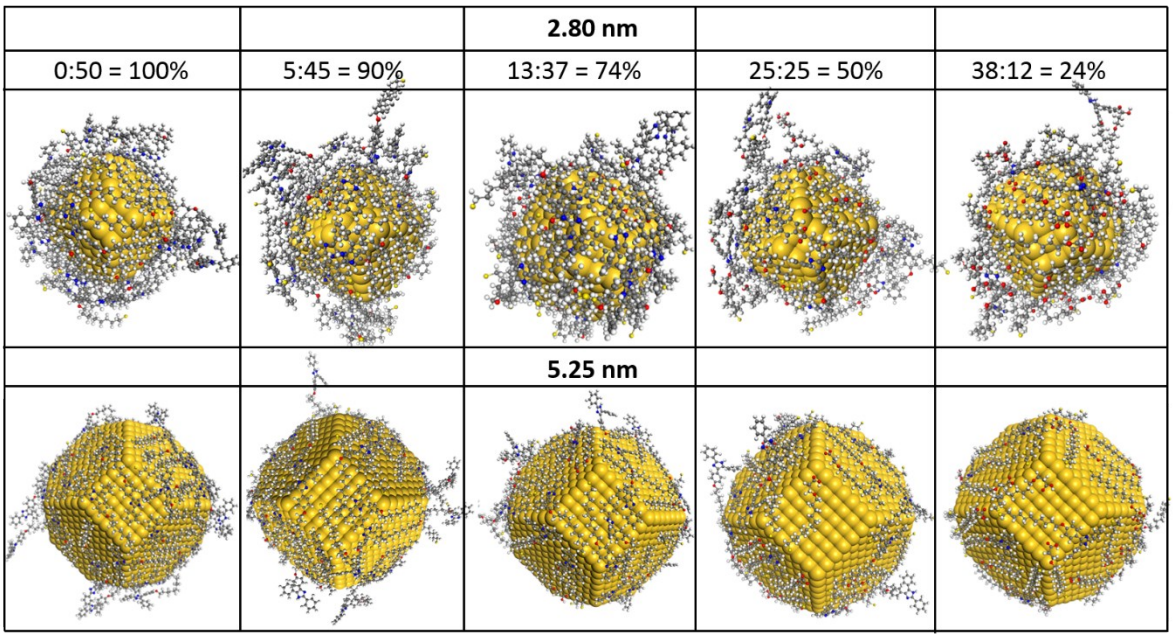

Figure S18: Relative molecule-to-surface orientation for different sized AuNPs with different ratios of PEG/Triphenylimidizone.

References

[1] K. J. Klabunde, R. M. Richards, *Nanoscale materials in chemistry*, John Wiley & Sons, Inc., Hoboken, New Jersey, 2009, 37-64.

[2] X. Liu, M. Atwater, J. Wang, Q. Huo, *Colloids and Surfaces B: Biointerfaces*, 2007, **58**, 3.

[3] W.C. Lin, S.H. Huang, C.L. Chen, C.C. Chen, D.P. Tsai, H.P. Chiang, *Appl. Phys. A*, 2010, **101**, 185.

[4] R.A. Harris, P.M. Shumbula, H. Van der Walt, *Langmuir*, 2015, **31**, 3934